

Photochemistry of Quinone-Bridged Amino Acids. Intramolecular Trapping of an Excited Charge-Transfer State¹

Guilford Jones, II* and Xiaohua Qian

Department of Chemistry and Center for Photonics, Boston University, Boston, Massachusetts 02215

Received: July 16, 1997; In Final Form: December 4, 1997

Linkages to amino acids that feature a chlorinated *p*-benzoquinone as a bridging group have been prepared by reaction of 2,5-dichloro-*p*-benzoquinone or chloranil with the free amine groups of alanine and proline. Electron-transfer capabilities of these peptide conjugates have been assessed through cyclic voltammetry and laser flash photolysis measurements. Phototransients are observed ($\lambda_{\text{max}} = 410 \text{ nm}$) that cannot be assigned to either triplet or radical anion intermediates normally associated with quinones. These intermediates are associated with novel biradical zwitterions that result from intramolecular trapping of an aminoquinone excited charge-transfer (CT) state.

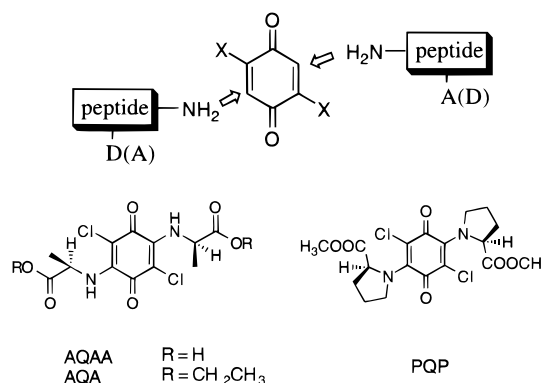
Introduction

Quinone subunits have figured prominently in the construction of covalent model compounds that mimic certain aspects of electron transfer that is observed in natural photosynthetic reaction centers.² In rare cases a quinone moiety has been provided as part of a peptide assembly that connects electron donor and acceptor groups (e.g., a quinone-substituted alanine linked to a porphyrin).³ As part of a study of photoactive peptides,⁴ and with a view to creating peptide chains that interact or “bundle” through hydrophobic or electrostatic contacts,⁵ we have considered the role that the *p*-benzoquinone structure might play in forging links between peptide segments. A quinone unit may serve as a covalent junction through symmetrical substitution of amine (terminal) groups supplied by peptide chains that are further modified with electron donors (D) and acceptors (A) as illustrated in Scheme 1. Several possible mechanisms of electron transfer could ensue from such an assembly including the separation of charge to remote positions on peptide pendants through preliminary steps of electron transfer involving the quinone moiety. A number of clever assemblies similar to these peptide designs, but involving other organic functionalities linked symmetrically to a central quinone unit, have been prepared and their photo- and electrochemical properties investigated.⁶

The assemblies that would derive from the covalent linkages implied in Scheme 1 take advantage of the Michael reaction of benzoquinones with primary and secondary amines.⁷ A variety of these reactions with amines are well-known, involving quinones with several different types of auxiliary substituent groups, X (halogen, alkyl). Reactions of benzoquinones with amino acids that lead to 2,5-substitution by an amine function on the quinone nucleus have been reported.^{8–10}

For the purpose of creating simple models for the study of quinone-linked peptides, chlorinated benzoquinones have been used in the present investigation for symmetrical substitution of the simple amino acids alanine and proline. These amino acids represent residues that favor or disfavor the formation of helices in peptides.¹¹ They also provide examples of substitution by both primary and secondary amine functional groups. Electrochemical and flash photochemical data are provided for the quinone–peptide link for the first time, and the appearance

SCHEME 1



of a phototransient that must be assigned to an unusual biradical-zwitterion intermediate are reported. Formation of this transient is consistent with the role of a low-lying charge-transfer state for amino-substituted quinones. Its mode of decay represents a hitherto unappreciated intramolecular pathway that leads to photocyclization of quinone and amino acid subunits.

Experimental Section

2,5-Dichloro-*p*-benzoquinone was purchased from Kodak and was used as received. Tetrachloro-1,4-benzoquinone (99%), L-proline, (99+%), L-alanine, and L-proline methyl ester (hydrochloride) (98%) were purchased from Aldrich and used without further purification. L-Alanine ethyl ester (hydrochloride salt) was obtained from Sigma and used as received. All the solvents used were A.R. grade. Silica gel from Baker Inc. (40 mm, 230–400 mesh) was employed as stationary phase for flash column chromatography. Aluminum-backed plates coated with silica gel 60-F254 (0.20 mm thickness, Doe & Ingall Inc.) were used for analytical thin-layer chromatography (TLC). Laser-desorption mass spectra were obtained using a PerSeptive Biosystems' Voyager biospectrometry workstation (MALDI-TOF mass spectrometer); a nitrogen laser, which operated at 337 nm, was used for sample ionization, and methanol was used as solvent for sample loading. A Rainin Dynamax C-18 reverse-phase column (4.6 mm i.d. × 25 cm, with particle size of 8 mm and pore size of 60 Å) was used for HPLC separations.

(*S,S*)-2,5-Bis[1'-carboxyethyl]amino]-3,6-dichloro-2,5-cyclohexadiene-1,4-dione (AQAA).⁸ A solution of chloranil (1 g, 3.9 mmol) in 55 mL of benzene was mixed with an aqueous solution of the sodium salt of L-alanine, which was prepared by adding L-alanine (0.87 g, 9.8 mmol) to a solution of 50 mL of aqueous NaOH (0.39 g, 9.8 mmol). After being stirred vigorously overnight, the two phases were separated and the aqueous layer was washed with another portion of 50 mL of benzene and then acidified to pH 3 after having been concentrated slightly. Ethyl acetate was used to extract the aqueous solution (3 × 50 mL); the combined ethyl acetate extracts were washed with saturated NaCl (2 × 50 mL). Thin-layer chromatography, developed in acetone acidified with acetic acid, showed only one product. After the organic extract over Na₂SO₄ was dried, the solvent was removed in vacuo. After recrystallization from ethyl acetate and hexanes, the product weighed 0.2 g, mp 165–167 °C. ¹H NMR (400 MHz, acetone-*d*₆): δ 7.35(br, 2H), 5.23 (m, 2H), 1.61 (d, 6H, *J* = 7.6 Hz).

(*S,S*)-2,5-Bis[1'-(ethoxycarbonyl)ethyl]amino]-3,6-dichloro-2,5-cyclohexadiene-1,4-dione (AQA).⁹ Following in part procedures for reaction of *p*-benzoquinone and chlorobenzoquinones with L-glycine ethyl ester,¹⁰ 2,5-dichloro-*p*-benzoquinone (2.5 g, 14 mmol) was dissolved in 60 mL of ethyl acetate with heating to 60 °C. L-Alanine ethyl ester (1.13 g, 9.4 mmol), freshly prepared from its hydrochloride salt in 15 mL of ethyl acetate, was added. The reaction mixture acquired a dark-red coloration immediately. Reaction was allowed to continue at 50 °C for 4 h and maintained at room temperature overnight. The solvent was evaporated in vacuo to yield a dark-red solid mass, which was purified by flash column chromatography on silica gel (ethyl acetate and petroleum ether gradient). Recrystallization of the eluted sample from ethyl acetate and petroleum ether afforded 0.856 g of product (62% yield) as rust-colored needles, mp 123–125 °C (reported mp 125–126 °C⁹). ¹H NMR (400 MHz, acetone-*d*₆): δ 7.35 (br, 2H), 5.21 (m, 2H), 4.24 (q, 4H, *J* = 7 Hz), 1.58 (d, 6H, *J* = 7.6 Hz), 1.27 (t, 6H, *J* = 7 Hz). HRMS (EI, 70 eV): *m/z* 406.0684 (M⁺, calcd 406.0698 for C₁₆H₂₀O₆N₂Cl₂).

(*S,S*)-2,5-Bis[1'-(methoxycarbonyl)pyrrolidino]-3,6-dichloro-2,5-cyclohexadiene-1,4-dione (PQP). Chloranil (1.64 g, 6.7 mmol) was dissolved in 100 mL of ethyl acetate upon heating to 60 °C. L-Proline methyl ester (16.7 mmol), prepared by treatment of the hydrochloride salt with triethylammonium chloride in chloroform, was added dropwise in 15 mL of ethyl acetate. The reaction mixture was allowed to react at 60 °C for 7 h and then let stand at room temperature overnight. After the solvent was evaporated under reduced pressure, the solid residue was then treated with 10 mL of methylene chloride. The byproduct, L-proline methyl ester hydrochloride, which was not soluble, was filtered. After evaporation of the resulting solution, the crude product was redissolved in acetone and mixed with 2 g of silica gel. The dried silica gel was then added to a 2 cm × 17 cm silica column. The eluent used was a gradient of petroleum ether and ethyl acetate, starting from 100% petroleum ether. The product that was eluted with 30% ethyl acetate in petroleum ether was dissolved in ethyl acetate and recrystallized on addition of hexanes to yield 0.752 g (30% yield, mp 60–61 °C) of the desired compound (light-brown color). ¹H NMR (400 MHz, CDCl₃): δ 5.11 (t, 2H, *J* = 7 Hz), 4.17 (m, 2H), 3.83 (m, 2H), 3.72 (s, 6H), 2.32 (m, 2H), 1.95 (m, 4H), 1.81 (m, 2H). ¹³C NMR (65.9 MHz, CDCl₃): δ 176.2 (2C), 172.4 (2C), 148.3 (2C), 105.3 (2C), 64.7 (2C), 56.0 (2C), 52.7 (2C), 30.8 (2C), 24.5 (2C). HRMS (EI, 70 eV): *m/z* 431.0793 (MH⁺, calcd 431.0777 for C₁₈H₂₁Cl₂N₂O₆).

Steady-State Photolysis of AQA. Preparative photolysis of AQA was carried out using a Hanovia immersion apparatus (450 W Hg Lamp). A Pyrex filter was used to cut off the absorption that is below 300 nm. Solutions were purged with Ar before and during the photolysis; cooling water kept the reaction temperature at 20 °C. A 5 mg sample of AQA was irradiated in 100 mL of methanol solution for 2 h. HPLC detection (20 min intervals) showed that the starting material was consumed. Absorption spectra (Figure 3) taken in 20 min intervals showed that the reaction was clean, with only one product found to be present having an absorption maximum at 381 nm. Isosbestic points were observed at 315 and 370 nm. After evaporation to dryness in *vacuo*, a yellow solid was obtained and identified as compound **II** (R = CH₂CH₃). ¹H NMR (400 MHz, CDCl₃): δ 4.93 (d, 1H, *J* = 9.2 Hz), 4.80 (m, 1H), 4.21 (m, 2H), 2.56 (s, 3H), 1.50 (d, 3H, *J* = 7.6 Hz), 1.28 (t, 3H, *J* = 6 Hz) ppm. MALDI-MS (337 nm excitation): *m/z* 359.97 (M⁺, calcd 360.03 for C₁₄H₁₄O₅N₂Cl₂). Spotted on a TLC plate, only one spot was found for the product (*R*_f = 0.3) when developed with 30% ethyl acetate in petroleum ether. However, compound **II** was found to decompose to a mixture of products on prolonged standing. Preparative HPLC or column chromatography of the product on silica also led to decomposition (NMR, TLC).

General Instrumentation. Measurements of pH were made on a Fisher Accumet pH meter; accuracy of the pH measurement was ±0.1. The absorption spectra were recorded on the Beckman DU-7 spectrophotometer. Flash photolysis experiments were carried out using a Nd:YAG laser system with λ/3 (355 nm) or λ/2 (532 nm) excitation. The basic design of the nanosecond laser flash photolysis system has been described previously.¹² The basic components included a Quantel YG-581-10 Nd:YAG laser controlled through a Kinetic Systems CAMAC interface crate, a LeCroy 6880A 1.35 gigasamples/s waveform digitizer, a LeCroy 6010 MAGIC controller, a pulsed xenon monitoring lamp, and a Hamamatsu R928 PMT. The data-fitting algorithm for analyzing transient decays employed the Marquart method, an iterative nonlinear least-squares fitting procedure. Dye solutions of 20 mM concentration were used in 2.2 cm × 1.0 cm rectangular Pyrex cells for laser flash photolysis experiments. Irradiation was carried out at room temperature. The solutions were deaerated prior to photolysis by purging with argon (ca. 25 min), unless specified otherwise.

Low-temperature phosphorescence spectra were attempted for AQA using a Perkin-Elmer MPF-44 A fluorescence spectrophotometer equipped with a mechanical chopper. Samples (50 mM) in 4 mm i.d. NMR tubes were placed inside a low-temperature Dewar flask filled with liquid nitrogen. The sample compartment was purged with nitrogen gas during the experiment. An excitation wavelength of 390 nm was chosen, and a 420 nm cutoff filter was used to eliminate arrival of scattered excitation light at the detector. No emission that could be ascribed to either fluorescence or phosphorescence was observed for AQA, with or without the operation of the mechanical chopper. The low-temperature organic glass matrixes used included methylcyclohexane (MCH) and ethanol/methanol (4:1).

Electrochemical Measurements. Voltammograms were recorded using a model 273A potentiostat/galvanostat (EG&G APR) controlled by the EG&G M270A (version 4.0) software package (scan rate: 1 mV/s to 5 V/s). The three-electrode system consisted of a glass carbon (GC) working electrode, an aqueous Ag/AgCl, KCl (saturated) reference electrode, and a Pt counter electrode. Typical experiments were performed on argon-purged 5 mL solutions of 1 mM quinone in acetonitrile

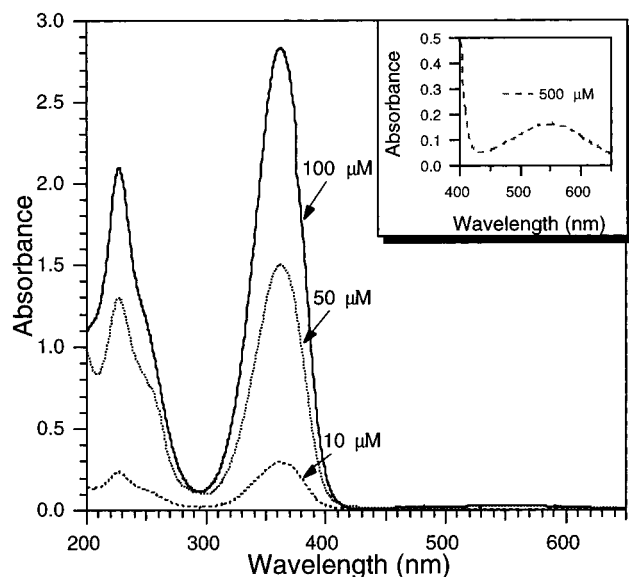


Figure 1. Absorption spectra for AQAA in acetonitrile/H₂O (5:1, v/v). Inset: absorption band in the long-wavelength region.

(dried and distilled over CaH₂), using 0.1 M tetrabutylammonium hexafluorophosphate (TBAH, Aldrich) as the supporting electrolyte. The oxidation of ferrocene in acetonitrile was used as reference (lithium perchlorate as supporting electrolyte) ($E_{1/2} = 0.37$ V vs SCE). The CV's were recorded using different scan rates, and the average $E_{1/2}$ (from four independent measurements) is reported.

Results and Discussion

Spectroscopic Properties of Quinone–Amino Acid Conjugates. Absorption spectral data for the selected quinones are shown in Figure 1 and in Table 1. The development of an intense band at about 350 nm in the ultraviolet is common for *p*-benzoquinone derivatives having amine substituents.^{13,14} The alterations of spectra from that observed for the parent 2,5-dichloro-*p*-benzoquinone ($\lambda_{\max} = 269$ and 327 nm, $\epsilon = 2.2 \times 10^4$ and 405 M⁻¹ cm⁻¹, respectively) have been observed with an array of aminoquinones and analyzed in terms of the enhancement and shift in energy for an allowed $\pi-\pi^*$ transition, through strong perturbation by amine substituents.¹³ This principal absorption (band 1) displays a small red shift for PQP compared with the alanine derivatives, presumably as the result of a stronger perturbation by the more substituted amine moiety.¹⁴ Subtle influences for the 350 nm transition were observed for the alanines; the free acid quinone conjugate, AQAA, showed a pronounced red shift of absorption for the quinone in water solution as the pH was altered from 1.5 to 7.0. On titration the absorption shift revealed a pK_a of 2.9, consistent with the charging of the amino acid moieties and a resultant perturbation of the electronic transition frequency (relative excited-state stabilization).

The pink-colored appearance of solutions is due to weak absorption by the quinone derivatives in the visible. The long-wavelength band (ca. 520 nm) is also the result of amine substitution. This band is shifted to the red on increase in solvent polarity (or for the more substituted amine functional group PQP), consistent with previous assignments of this transition for amino-substituted quinones to an intramolecular charge-transfer transition.^{13,14} Notably, the extinction coefficient for this long-wavelength band is quite small (Table 1), the result of steric crowding of quinone ring substituents (e.g., -NR₂, -Cl), which force the amine functionality (lone-pair electrons)

out of formal conjugation with the quinone π system (vide infra). Neither fluorescence nor phosphorescence emission was observed for the quinone derivatives at room temperature or at 77 K.

Cyclic Voltammetry. The quinone derivatives in dry acetonitrile were reduced at moderately negative potentials associated with reversible one- and two-electron reduction processes (Table 1). The second reduction wave was overlapped with the first reduction wave for AQAA, reflecting the involvement of the free acid functional groups in chemistry following two-electron reduction. The values for the one-electron half-wave potentials are consistent with those obtained for other substituted quinones for which the pattern is to move to more positive potentials with the addition of electron-withdrawing chlorine substituents and to more negative potentials on substitution with electron-donating amine groups.^{15,16}

Laser Flash Photolysis. Phototransients were observed on flash photolysis of AQA and AQAA in several solvents. Excitation could be carried out at either 355 or 532 nm (tripled and doubled Nd:YAG laser wavelengths), although use of the longer wavelength required much higher concentrations of quinone (note the low relative absorptivity in Table 1), which obscured critical wavelengths. The common transient, observed under virtually all conditions explored, displayed a peak wavelength of 400 nm and decayed in the microsecond time domain. Representative spectra resulting from flash photolysis of AQA and AQAA are shown in Figure 2.

The transient decays monitored at 400 nm, which were cleanly first order, provided lifetimes that were examined as a function of medium conditions for AQA (Table 2). Aeration of samples resulted in spectra that were identical, although faster decay times were observed (4- to 10-fold effects), consistent with the quenching of phototransients by molecular oxygen. Transient decays were not accelerated as a function of solvent polarity (acetonitrile versus methylene chloride versus ethyl acetate). Decay was moderately faster for photolysis of isopropyl alcohol (IPA) solutions of AQA, but this influence was not clearly due to the role of IPA as hydrogen-atom donor. Indeed, the most compelling comparison was that transient depletion was accelerated moderately for all hydroxylic media (alcohols, addition of water; see Table 2). An isotope effect of 1.5 was measured on comparing rates of decay of the 400 nm species in methanol with rates in methanol-*d*₄. Notably, the conjugate having the proline amine substituent, PQP, failed to show similar phototransient behavior (only photobleaching near 350 nm coincident with the laser pulse).

An effort was made first to assign the 400 nm transient to the triplet state of the conjugates. The low-lying triplet is in fact the excited-state intermediate most commonly observed for *p*-benzoquinones, although in a few studies formation of triplets observable in the nanosecond to millisecond time domain has been shown to be compromised by substitution with amino groups.^{13,17} It was reasoned that a long-lived triplet of a readily reduced quinone would participate in diffusion-limited electron transfer if an electron donor is added.^{18,19} As an electron-transfer probe, *N*-acetyl-*N,N'*-dimethyl-*p*-phenylenediamine [CH₃CONHC₆H₄N(CH₃)₂], having $E(D^{+/0}) = 0.53$ V vs SCE and a readily observed transient radical cation ($\lambda_{\max} = 540$ nm),¹⁹ was used as potential donor for quenching a putative AQA triplet. In the event of photolysis of the quinone in the presence of 0.1–1.0 mM AcDMPD in Ar-purged methanol, only the 400 nm species was in evidence ($\tau = 1.0$ μ s). For this test a favorable thermodynamic driving force ($\Delta G_{\text{et}} = -0.68$ eV) for triplet quenching via electron transfer was estimated on the

TABLE 1: Absorption and Electrochemical Properties of Quinone-Linked Peptides

	solvent	band 1		band 2		$E_{1/2}$ (V vs SCE) ^a
		λ (nm)	$\epsilon \times 10^{-4}$ (M ⁻¹ cm ⁻¹)	λ (nm)	ϵ (M ⁻¹ cm ⁻¹)	
AQA	CH ₂ Cl ₂	354	3.02	524	200	-0.64(-1.2)
	MeOH	351	2.90	522	270	
	CH ₃ CN	351	2.51	520	274	
	CH ₃ CN/H ₂ O ^b (pH 7.0)	353	2.90			
AQAA	CH ₂ Cl ₂	352	2.69			-0.65
	EtOH	354	2.76			
	CH ₃ CN	350	2.40	524	232	
	CH ₃ CN/H ₂ O ^b (pH 7.0)	363	2.58	555	262	
	CH ₃ CN/H ₂ O ^b (pH 1.5)	357	2.70	555	262	
PQP	CH ₃ CN	364	1.13	540	438	-0.64(-1.0)
	CH ₂ Cl ₂	367	1.08	527	535	

^a CH₃CN with TBAH as supporting electrolyte. ^b 3:1 (v/v).

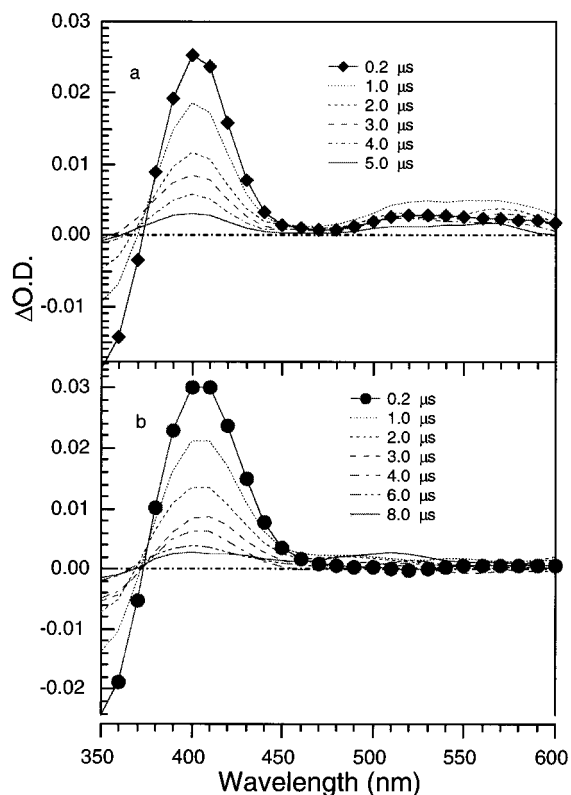


Figure 2. Transient absorption obtained on laser flash photolysis of (a) 20 μ M AQAA in acetonitrile and (b) 20 μ M AQA in methanol. $\lambda_{exc} = 355$ nm.

TABLE 2: Lifetimes of the 400 nm Transient Observed on Laser Flash Photolysis of AQA in Different Solvents ($\lambda_{exc} = 355$ nm)^a

solvent	τ (μ s)	
	Ar-purged solution	air-saturated solution
dichloromethane	4.69 \pm 0.13	0.61 \pm 0.04
ethyl acetate	3.14 \pm 0.10	0.30 \pm 0.02
2-propanol	2.00 \pm 0.06	
methanol	1.57 \pm 0.03	
methanol- <i>d</i> ₄	2.34 \pm 0.08	
acetonitrile	3.35 \pm 0.08	0.24 \pm 0.02
acetonitrile/H ₂ O ^b	1.45 \pm 0.04	0.44 \pm 0.02

^a Decay times from single-exponential fits. ^b 3:1 (v/v).

basis of the Weller equation:¹⁸ $\Delta G_{et} = nF[E^\circ(D^{+}/D) - E^\circ(A/A^{-})] - E_{00} - e^2/(\epsilon r)$, where E° values are the half-wave potentials provided for AcDMPD and AQA, the excitation energy E_{00} , is estimated (1.8 eV),²⁰ and the Coulombic term is evaluated at 0.05 eV (CH₃CN solvent).¹⁸

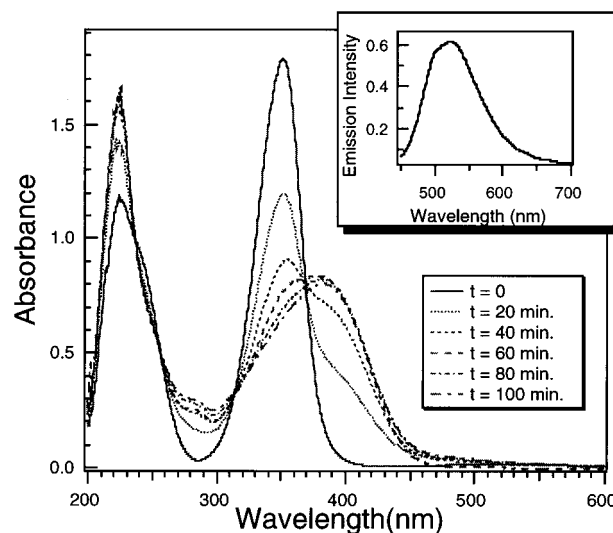
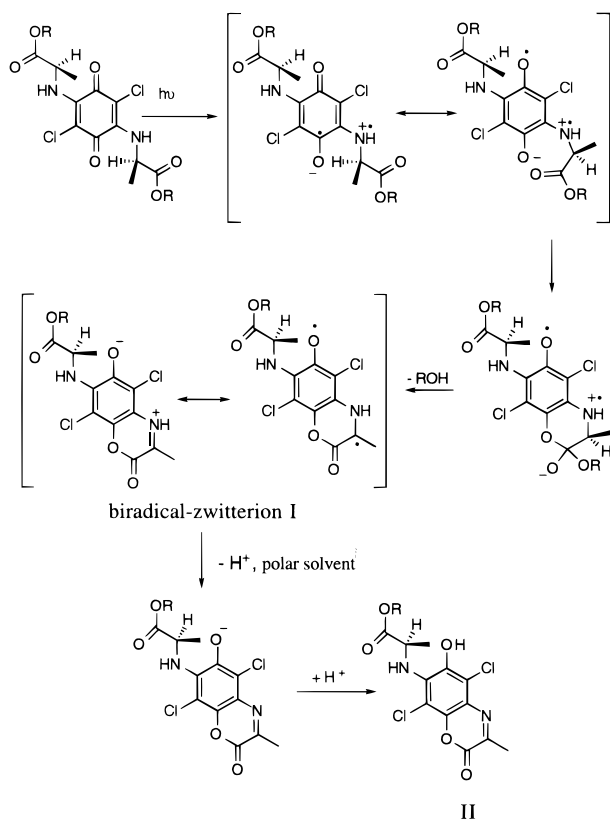


Figure 3. Absorption spectra for 60 μ M AQA in Ar-purged methanol before and after steady irradiation (Hanovia photoreactor, Pyrex filter). Inset: emission spectrum of product (CH₃OH; $\lambda_{exc} = 380$ nm).

Steady-State Photolysis: A Mechanism for Photocyclization. Irradiation of AQA or AQAA with an Hg lamp resulted in spectral changes that are illustrated in Figure 3. The photodecomposition of AQA in methanol was examined in detail. Most conspicuous was the formation on photolysis of a single product (note the isosbestic point in Figure 3) that absorbed at longer wavelengths and displayed a bright-green fluorescence. The photoproduct, although somewhat unstable and difficult to purify by chromatographic means, could be obtained in nearly pure form and analyzed by NMR and matrix-assisted laser-desorption mass spectrometry (MALDI). The spectral data were consistent with a formula of the original quinone conjugate minus the elements of ethanol ($m/e = 359.97$). Most distinctive in the proton NMR spectrum was the appearance of resonances associated with a single methyl group at δ 2.6 ppm and the loss of an N-H proton. These features have their origin in the side chain (CH₃) of the alanine moiety and one NH group in the original AQA structure.

Other possible fragmentation, ring substitutions, and rearrangements known for other quinones including aminoquinones (vide infra)¹³ could be discounted on the basis of the NMR and MS data. The data are most consistent with the assignment of structure **II** to the photoproduct. Useful also in confirming this assignment were the UV-vis and fluorescence data, which revealed a significant solvatochromism for the photoproduct. For methanol solutions, $\lambda_{max} = 380$ nm and λ_f (max) = 523 nm (Figure 3). A more intense fluorescence was observed for

SCHEME 2

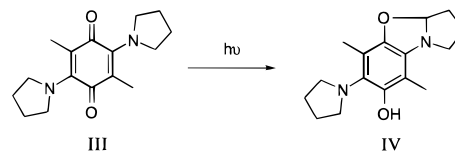


methylene chloride solutions, and $\lambda_{\text{max}} = 375$ nm and $\lambda_{\text{f}} (\text{max}) = 482$ nm for **II** in the less polar solvent. These trends mimicked the spectral positions and medium sensitivity associated with the well-known 7-aminocoumarin chromophore that is associated with the coumarin family of laser dyes.²¹

The phototransient experiments and the identification of photoproduct for AQA combine to reveal a novel mechanism of rearrangement–fragmentation for the quinone conjugates. As shown in Scheme 2, excitation leads to the low-lying intramolecular charge-transfer state (ICT), a species forced into a twisted conformation because of steric interaction of ring substituents and associated with the weakly allowed long-wavelength transition for the quinones ($\lambda_{\text{max}} = \text{ca. } 520$ nm).²² This zwitterionic species is juxtaposed with the side chain provided by amino acid groups in such a way to favor trapping by a pendant carbonyl moiety. Cyclization and elimination of ethanol lead to intermediate **I**. The latter displays a chromophore (the 400 nm transient in Figure 2) similar to that observed for semiquinone intermediates ($\lambda_{\text{max}} = \text{ca. } 400$ nm).^{13,23} This species would be expected to react readily with oxygen¹³ but be sufficiently stable not to be intercepted by a moderate hydrogen-donor solvent, IPA. The behavior of **I** is further understood in terms of the polar character that is probable for this structure (i.e., the importance of the zwitterionic form; see Scheme 2). Deprotonation–reprotonation of **I** results in formation of product **II**. The last steps of proton transfer are expected to be sensitive to the availability of hydroxylic solvents, thus the solvent effects that are observed for the 400 nm transient (Table 2).

The absence of the cyclization–elimination photochemical pathway for PQP can be understood in terms of the photochemistry of analogous aminoquinones. An examination of models suggests that the ring-closure step in which intermediate **I** is formed (Scheme 2) is prohibited for PQP because the three

linked rings are required to achieve a nearly planar arrangement, a step made more difficult by Cl ring substituents. In lieu of formation of **I**, the most likely alternative mechanism is proton transfer for the ICT excited state for PVP, which leads to a biradical capable of another type of ring closure. This pathway is illustrated below in the reported²⁴ transformation of the bis-(pyrrolidiny) quinone, **III** \rightarrow **IV**.



Other interesting examples of charge-transfer intermediates that are responsible for rearrangement or fragmentation reactions include cyclization analogous to **III** \rightarrow **IV** for 2-chloro-3-(dimethylamino)-1,4-naphthoquinone²⁵ and the alternative electron-transfer mechanism proposed for Norrish type II photoelimination of α -aminoketones.²⁶

In summary, quinone conjugates of simple amino acids alanine and proline act as reversible electron-transfer acceptors. Their photochemistry is dominated by intramolecular electron-transfer reactions that occur via a low-lying charge transfer (ICT) excited state. Alanine conjugates lead to unusual biradical-zwitterion intermediates (**I**), readily observed phototransients ($\lambda_{\text{max}} = 400$ nm) that appear in the microsecond time domain, that result from intramolecular trapping by the carboxyl functions of amino acid pendant groups. This cyclization reaction is demonstrated in the formation of the coumarin photoproduct **II**.

Acknowledgment. We thank the Division of Chemical Sciences, Office of Basic Energy Sciences of the U.S. Department of Energy for financial support of this work.

References and Notes

- (1) Paper 7 in the series Photoactive Peptides.
- (2) See, for example, the following. Gust, D.; Moore, T. A.; Moore, A. L. *Acc. Chem. Res.* **1993**, *26*, 198. Wasielewski, M. R. *Chem. Rev.* **1992**, *92*, 435. Ohkohchi, M.; Takahashi, A.; Mataga, N.; Okada, T.; Osuka, A.; Yamada, H.; Maruyama, K. *J. Am. Chem. Soc.* **1993**, *115*, 12137.
- (3) Tamiaki, H.; Maruyama, K. *Chem. Lett.* **1993**, 1499.
- (4) Jones, G., II.; Lu, L. N.; Vullev, V.; Gosztola, D. J.; Greenfield, S. R.; Wasielewski, M. R. *Bioorg. Med. Chem. Lett.* **1995**, *5*, 2385. Jones, G., II.; Farahat, C. W.; Oh, C. *J. Phys. Chem.* **1994**, *98*, 6906. Jones, G., II.; Farahat, C. W. *Res Chem. Intermed.* **1994**, *20*, 855. Jones, G., II.; Vullev, V.; Braswell, E. H.; Zhu, D. *J. Phys. Chem.*, submitted.
- (5) Jones, G., II.; Vullev, V. I. In preparation.
- (6) Hable, C. T.; Crooks, R. M.; Valentine, J. R.; Giasson, R.; Wrighton, M. S. *J. Phys. Chem.* **1993**, *97*, 6060. Smith, D. S.; Lane, G. A.; Wrighton, M. S. *J. Phys. Chem.* **1988**, *92*, 2616.
- (7) Finley, K. T. In *The Chemistry of the Quinonoid Compounds*; Patai, S., Rappoport, Z., Eds.; John Wiley & Sons: New York, 1988; Vol. 2, Part 1, p 537.
- (8) Aldiaturi, C. E.; Otero, V.; Anzola, F.; Rosillo, F. *Acta Cient. Venez.* **1982**, *33*, 348.
- (9) Ioffe, I. S.; Khavin, Z. Y. *Zh. Obshch. Khim.* **1954**, *54*, 521, 527.
- (10) Foster, R.; Kulevsky, N.; Wanigasekera, S. *J. Chem. Soc., Perkin Trans 1* **1974**, 1318.
- (11) Branden, C.; Tooze, J. In *Introduction to Protein Structure*; Garland Publishing Inc.: New York, 1991; p 14.
- (12) Malba, V.; Jones, G., II.; Poliakov, E. D. *Photochem. Photobiol.* **1985**, *42*, 451.
- (13) Bruce, J. M. In *The Chemistry of Quinonoid Compounds*; Patai, S., Ed.; John Wiley & Sons: New York, 1974; Part 1, p 472.
- (14) Wallenfels, K.; Draber, W. *Tetrahedron* **1964**, 1889. Ramachandran, M. S.; Singh, U. C.; Subbaratnam, N. R.; Kelkar, V. K. *Proc. Indian Acad. Sci.* **1979**, *88*, 155.

- (15) Chambers, J. Q. In *The Chemistry of Quinonoid Compounds*; Patai, S., Rappoport, Z., Eds.; John Wiley & Sons: New York, 1988; Vol. 2, p 719.
- (16) Klopman, G.; Doddapaneni, N. *J. Phys. Chem.* **1974**, *78*, 1820.
- (17) Dearman, H. H.; Chan, A. *J. Chem. Phys.* **1966**, *44*, 416.
- (18) Kavarnos, G. J.; Turro, N. J. *Chem. Rev.* **1986**, *86*, 401.
- (19) Jones, G., II.; Lu, L. N.; Fu, H.; Gosztola, D. J.; Greenfield, S. R.; Wasielewski, M. R. In preparation.
- (20) In the absence of phosphorescence data, E_{00} , the triplet energy, was estimated based on the onset of ground-state absorption and a reasonable estimation of the singlet-triplet separation (and compared with triplet energies noted for other quinones);¹³ see the following. Qian, X. Ph.D. Dissertation, Boston University, Boston, MA, 1998.
- (21) Jones, G., II. In *Dye Laser Principles: with Applications*; Duarte, F. J., Hillman, L. W., Eds.; Academic Press: New York, 1990; Chapter 7. Jones, G., II; Jackson, W. R.; Choi, C. *J. Phys. Chem.* **1985**, *89*, 294.
- (22) Molecular mechanics (MOPAC) calculations for AQA show energy minima for angles of rotation for the amine moiety (the N-C bond with respect to the quinone ring) near 90°.
- (23) Bridge, N. K.; Porter, G. *Proc. R. Soc. London* **1958**, *A244*, 259, 276.
- (24) Cameron, D. W.; Giles, R. G. F. *J. Chem. Soc. C* **1968**, 1461.
- (25) Gritsan, N. P.; Bazhin, N. M. *Izv. Akad. Nauk SSSR, Ser. Khim.* **1980**, 1275. Gritsan, N. P.; Bazhin, N. M. *Izv. Akad. Nauk SSSR, Ser. Khim.* **1981**, 118, 280.
- (26) Padwa, A.; Eisenhardt, W.; Gruber, R.; Pashayan, D. *J. Am. Chem. Soc.* **1969**, *91*, 1857.